

Detailed spectral study of an ultra-luminous compact X-ray source M81 X-9 in the disk dominated state

Naoko TSUNODA,^{1,2} Aya KUBOTA,¹ Masaaki NAMIKI,³ Masahiko SUGIHO,⁴
Kiyoshi KAWABATA,² and Kazuo MAKISHIMA^{1,5}

¹*Institute of Physical and Chemical Research (RIKEN), 2-1 Hirosawa, Wako, Saitama 351-0198*

²*Department of Physics, Tokyo University of Science, 1-3 Kagurazaka, Shinjuku-ku, Tokyo 162-8601*
tsunoda@crab.riken.jp

³*Department of Earth and Space Science, Osaka University,*
1-1 Machikaneyama-cho, Toyonaka, Osaka 560-0043

⁴*NEC TOSHIBA Space Systems, Ltd. 1-10, Nissin-cho, Fuchu, Tokyo, 183-8551, Japan*

⁵*Department of Physics, University of Tokyo, 7-3-1 Hongo, Bunkyo-ku, Tokyo 113-0033*

(Received 2006 February 24; accepted 2006 October 12)

Abstract

We report on the results of detailed spectral studies of the ultra-luminous X-ray source (ULX), M81 X-9 (Holmberg IX X-1), made with XMM-Newton on 2001 April 22 and with ASCA on 1999 April 6. On both occasions, the source showed an unabsorbed 0.5–10 keV luminosity of $\sim 2 \times 10^{40}$ erg s⁻¹ (assuming a distance of 3.4 Mpc) and a soft spectrum apparently represented by a multi-color disk model with an innermost disk temperature of 1.3–1.5 keV. Adding a power-law model further improved the fit. However, as previously reported, the high luminosity cannot be reconciled with the high disk temperature within a framework of the standard accretion disk radiating at a sub-Eddington luminosity. Therefore, we modified the multi-color disk model, and allowed the local disk temperature to scale as $\propto r^{-p}$ on the distance r from the black hole, with p being a free parameter. We then found that the XMM-Newton and the ASCA spectra can be both reproduced successfully with $p \sim 0.6$ and the innermost disk temperature of 1.4–1.8 keV. These flatter temperature profiles suggest deviation from the standard Shakura-Sunyaev disk, and are consistent with predictions of a slim disk model.

Key words: accretion, accretion disks—black hole physics—X-rays: individual (M81 X-9, Holmberg IX X-1)—X-rays: stars

1. Introduction

Nearby spiral galaxies often host ultra-luminous compact X-ray sources (hereafter ULXs; Makishima et al. 2000), with X-ray luminosities reaching 3×10^{39} – 10^{40} erg s⁻¹. Although they require black hole masses of 20–100 M_{\odot} or more by considering the Eddington limit, L_E , it is not obvious whether such massive stellar black holes can be created as an end point of evolution of massive stars. Thus, there are still extensive arguments on the nature of the ULXs. Thanks to ASCA, a great leap has been achieved in our understanding of 1–10 keV spectra of a dozen ULXs. As reported by many authors (Okada et al. 1998; Makishima et al. 2000, and references therein), spectra of a majority of the ASCA sample have been reproduced by so-called multi-color disk (MCD) model (DISKBB in XSPEC¹; Mitsuda et al. 1984; Makishima et al. 1986), while others are described with a power-law model. The MCD model approximates emission from a geometrically thin, radiation dominated standard accretion disk (Shakura & Sunyaev 1973), and successfully describes the dominant soft spectral component of Galactic/Magellanic black hole binaries (hereafter BHB)

in the high/soft state. In addition, spectral transitions between the disk dominant type and the power-law dominant type states have been observed in several ULXs (e.g., Kubota, Done, Makishima 2002; La Parola et al. 2001). These spectral characteristics of ULXs have thereby reinforced their candidacy as accreting black holes.

In spite of the successful application of the MCD model to the ULX spectra, there still remain three self inconsistencies. One is known as “too high T_{in} ” problem that the values of the innermost disk temperature, T_{in} , obtained from the disk-dominant ULXs (typically 1–2 keV; Makishima et al. 2000) are significantly higher than those of BHBs (0.5–1.2 keV), even though higher-mass black holes should have lower values of T_{in} as $T_{in} \propto M^{-1/4}$ under the standard-disk picture (e.g., Makishima et al. 2000). The second one is known as “variable r_{in} ” problem: the inner disk radius, r_{in} , of ULXs are reported to vary as $r_{in} \propto T_{in}^{-1}$ (Mizuno, Kubota, Makishima 2001), in contradiction to the case of high-state BHBs in which r_{in} is generally constant at a value consistent with the radius of last stable orbit around the central black hole (e.g., Makishima et al. 1986; Tanaka & Lewin 1995; Ebisawa et al. 1993; 1994). The last problem is that the ULXs luminosity at which the spectral transition occurs, $\sim 10^{39}$ erg s⁻¹, is too high to be considered as the classical high-low state tran-

¹ <http://heasarc.gsfc.nasa.gov/docs/xanadu/>

sitions of BHBs which generally occurs at several percent of L_E

The “too high T_{in} ” problem might be solved within the framework of standard accretion disks, by invoking extreme assumptions. For example, a rapid black hole rotation could increase T_{in} (Makishima et al. 2000) but the effect may not be sufficient to explain the ULX spectra (Ebisawa et al. 2003). Alternatively, the values of T_{in} could increase if the color-to-effective correction factor κ took a very high values as 3–5, for some unknown reasons, but this would contradict the canonical value of $\kappa = 1.5$ –2.0 suggested theoretically (Shimura & Takahara 1995; Davis et al. 2005) and observationally (Makishima et al. 2000). Furthermore neither of these “solutions” may solve the second and third problems.

Considering these difficulties, accretion flows in ULXs may be significantly deviated from the description of standard accretion disks, even though the emergent spectra look rather alike. Actually, when the mass accretion rate, \dot{M} , increases and the luminosity becomes closer to L_E , the disk structure is expected to change from the standard disk to a slim disk (e.g., Abramowicz et al. 1988; Watarai et al. 2000). The slim disk is predicted to have a significantly higher inner temperature than the standard accretion disk, and its apparent r_{in} (when fitted with the MCD model) is expected to vary roughly as $\propto T_{in}^{-1}$ (Watarai et al. 2000) just as is observed. These explain away the first and second problems, respectively (e.g., Mizuno, Kubota, Makishima 2001; Watarai, Mizuno, Mineshige 2001). Further, invoking the slim disk implies that the radiation luminosity is close to L_E , thus solving the third problem. Therefore, the slim disk scenario can potentially solve the three problems associated with the interpretation of disk dominated ULXs.

While the radiation-dominated standard disk is characterized by a local temperature varying as $T(r) \propto r^{-3/4}$ (r being the distance from the central black hole), the temperature profile of the slim disk is predicted to be flatter than this as $T(r) \propto r^{-0.5}$. The different temperature profiles are expected, in turn, to give subtle differences to the overall disk spectra. This effect may be described by so-called p -free disk model (a local model for XSPEC²; Mineshige et al. 1994; Hirano et al. 1995; Kubota & Makishima 2004), it assumes that the spectrum is composed of multi-temperature blackbody emission, where the local temperature $T(r)$ at a radius r is given by $T(r) = T_{in}(r/r_{in})^{-p}$, with p being a positive free parameter. Using the ASCA and RXTE data of Galactic/Magellanic BHBs, it has been confirmed that p takes a value consistent with the standard value, 3/4, when the objects are considered to reside in the standard-disk state with constant values of r_{in} (Kubota et al. 2005), and that p becomes smaller than 3/4 in a supposedly slim disk state (Kubota & Makishima 2004; Abe et al. 2005).

In the present paper, we apply the p -free disk model analysis to X-ray spectra of M81 X-9 in the disk dominant state, obtained with XMM-Newton on 2000 April

22 and with ASCA on 1999 April 6, in search for the expected spectral deviation from the standard disk. At a distance of 3.4 Mpc (Georgiev et al. 1991), this source is an extensively studied ULX associated with the dwarf galaxy Holmberg IX, which is a close companion to M81. Through previous snapshot observations with ASCA in 1993–1999, its unabsorbed 0.5–10 keV luminosity was found in $(6\text{--}20) \times 10^{39}$ erg s⁻¹ assuming an isotropic emission. Until 1998, the source kept a relatively low luminosity of $\sim 6 \times 10^{39}$ erg s⁻¹, with a single power-law spectrum of photon index $\Gamma \sim 1.4$ (Ezoe, Iyomoto, Makishima 2001). In the 1999 observation, the source was reported to have made a spectral transition to a disk-dominant state with $T_{in} = 1.24$ keV, together with an increased luminosity of $\sim 1.8 \times 10^{40}$ erg s⁻¹ (La Parola et al. 2001). Good XMM-Newton observations of M81 X-9 were performed three times by 2002. In 2001, its luminosity and spectral shape were almost the same as those obtained in the 1999 ASCA observation (Sugihō 2003). In the 2002 observations, the source became slightly fainter with an unabsorbed 0.3–10 keV luminosity of $L = 1.1\text{--}1.3 \times 10^{40}$ erg s⁻¹, and its spectrum returned to the power-law dominant state with a hint of cool MCD component (Miller, Fabian, Miller 2004).

Out of these multiple datasets, here we select two particular ones for our p -free study, namely the 1999 ASCA data and the 2001 XMM-Newton data, because the object was clearly in the disk dominant state on these occasions. These data sets are expected to give a significantly smaller values of p than that of standard disk, 3/4, if the slim disk is realized. These are the same data as analyzed already by La Parola et al. (2001) and Sugihō (2003), respectively.

2. Observations and Data Reduction

The present XMM-Newton observation of M81 X-9 was performed for 127.9 ks on 2001 April 22 (observation ID of 0111800101), with the three detectors of the European Photon Imaging Camera (EPIC). The two MOS cameras were operated in full frame mode, and the PN camera with the medium filter was operated in small window mode. We retrieved the data from the XMM-Newton public archive³, and used only MOS-1 data for the spectral study, since the source fell in the chip boundary of MOS-2 and outside the field of view (FOV) of the PN camera. The event file was reprocessed and filtered with the XMM-Newton Science Analysis Software (SAS v6.0.0). Utilizing light curves of source-free regions from the MOS-1 data, we rejected intervals with high background levels, and obtained a net exposure of 79.7 ks for the MOS-1 camera.

Figure 1 shows a MOS-1 image in the range of 0.5–10 keV. The source is thus located at 12'5" off the center of the MOS-1 FOV. Using a SAS task XMMSELECT (v6.0.1), the MOS-1 events with patterns 0 to 12 were extracted from a circular region of 50'' radius around the position of M81 X-9, $(\alpha, \delta) = (09^{\text{h}}57^{\text{m}}53^{\text{s}}, +69^{\circ}03'47'')$. Background events were accumulated over a source-free region with a

² <http://heasarc.gsfc.nasa.gov/docs/xanadu/xspec/models/diskpbb.htm><http://xmm.vilspa.esa.es/>

1.7 radius, at a position $(\alpha, \delta) = (09^{\text{h}}57^{\text{m}}43^{\text{s}}, +68^{\circ}59'24'')$. The on-source and the background regions are indicated in figure 1. Figure 2 shows the 0.5–10 keV light curve of M81 X-9. There is no significant intensity variations beyond the Poisson noise, with a typical upper limit of 10%. The average count rate, 0.424 ± 0.004 cts s^{-1} , roughly corresponds to a 0.5–10 keV flux of 1.4×10^{-11} erg s^{-1} cm^{-2} .

Since M81 X-9 is located close to the edge of MOS-1 FOV, its spectral analysis might be subject to calibration uncertainties. Therefore, we analyzed three data sets of a calibration target, the supernova remnant G21.5-09 which shows a power-law spectrum, one acquired near the FOV center and the others 11:12 and 13:02 off. As detailed in Appendix, we have confirmed that the spectra of such off-axis sources can be studied with a high reliability. Though the off-axis data may yield slightly harder spectrum than the on-axis ones, the difference in the photon index is less than ~ 0.1 (see figure6 in Appendix).

To compare with the XMM-Newton result on the disk dominant state, we also reanalyzed the ASCA SIS (Solid state Imaging Spectrometer) data of M81 X-9 obtained on 1999 April 6. We used the screened data set provided by the DARTS science archive⁴ with a net exposure of 33 ks. The source spectra were accumulated over a circular region centered on the source, with a radius of 2'9, and the background spectra were created using blank sky data. The criteria of the data screening are as follows: a) the object be at least 10° above the night Earth's limb or at least 20° above the bright Earth's limb; c) the cutoff rigidity (COR) of cosmic rays be greater than 6 GeV c^{-1} ; and d) the time after day night transition be greater than 100 s. The 0.5–10 keV count rate of M81 X-9 was 0.326 ± 0.003 and 0.272 ± 0.003 cts s^{-1} with SIS0 and SIS1, respectively. The implied 0.5–10 keV flux, approximately 1.3×10^{-11} erg s^{-1} cm^{-2} , is close ($\sim 93\%$) to that of the 2001 XMM-Newton data.

3. Data Analysis and Results

3.1. Analysis of the XMM-Newton data with canonical models

A left panel of figure 3 shows a MOS-1 spectrum of M81 X-9 in the range of 0.5–10 keV. Using a SAS task EPATPLOT, the MOS-1 data were confirmed to be free from photon pile-up effects. Following the standard modeling of ULXs (e.g., Makishima et al. 2000), we first examined the spectrum with a single power-law model and the MCD model, and obtained the fitting results as shown in Table 1. Here, the response matrices were created by RMFGEN and ARFGEN (v6.0.1), and the spectral fitting was performed with the software package XSPEC 11.2.0. The model was subjected to photoelectric absorption by a hydrogen column which is left free to vary. The single power-law fit was far from acceptable, with $\chi^2/(\text{d.o.f}) = 574.1/335$. The single MCD fit was much more successful, and yielded the parameters which are very similar to the ASCA results in 1999 reported by La

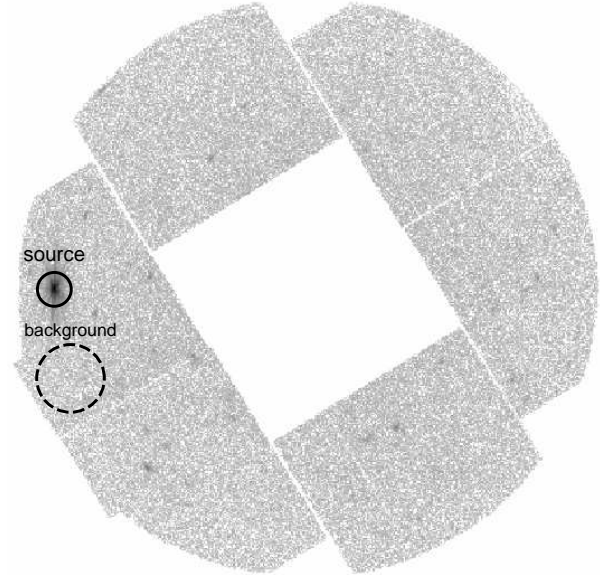


Fig. 1. A 0.5–10 keV unsmoothed MOS-1 image of the M81 X-9 field obtained on 2001 April 22. The source region and the background region are shown with a solid circle and a dotted circle, respectively. The background is included.

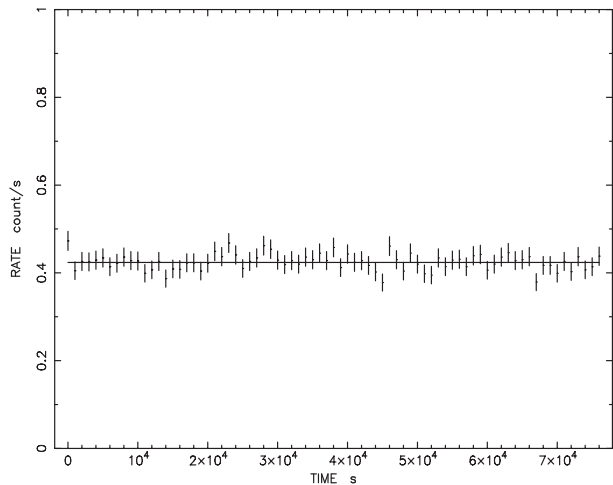


Fig. 2. The 0.5–10 keV MOS-1 light curve of M81 X-9, plotted with a time bin of 1 ks. A solid line indicates the best fit constant.

⁴ <http://www.darts.isas.jaxa.jp/index.html>

Parola et al. (2001). However, the fit still remained unacceptable with $\chi^2/(\text{d.o.f}) = 427.4/335$.

We hence fit the data with an MCD plus power-law model, as is done for galactic BHBs in the high state. This two-component model has successfully reproduced the observed spectrum with $\chi^2/(\text{d.o.f}) = 359.4/333$. As shown in Table 1, the best-fit model implies an absorbed 0.5–10 keV flux of $1.4 \times 10^{-11} \text{ erg s}^{-1} \text{ cm}^{-2}$, in which the MCD component accounts for $\sim 60\%$. The unabsorbed luminosity in the same band is obtained as $2.3 \times 10^{40} \text{ erg s}^{-1}$, assuming an isotropic emission. The MCD parameters, T_{in} and r_{in} , have been measured to be 1.45 keV and $(160 \pm 12) \cdot \alpha \text{ km}$ with $\alpha = \sqrt{\cos 60^\circ / \cos i}$ (i being the inclination angle of the disk), respectively. The true inner radius of the disk is calculated as $R_{\text{in}} = (190 \pm 15) \cdot \alpha \text{ km}$, by using a relation of $R_{\text{in}} = \xi \kappa^2 r_{\text{in}}$, when $\xi = 0.41$ is a correction factor for the inner boundary condition (Kubota et al. 1998) and $\kappa = 1.7$ is a spectral hardening factor (Shimura & Takahara 1995). The disk bolometric luminosity is estimated as $L_{\text{bol}} = 1.5 \times 10^{40} \cdot \alpha^2 \text{ erg s}^{-1}$ through a relation of $L_{\text{bol}} = 4\pi\sigma r_{\text{in}}^2 T_{\text{in}}^4$ (Makishima et al. 1986), with σ the Stefan-Boltzman constant. When the 0.5–10 keV unabsorbed power-law luminosity, $8.7 \times 10^{39} \text{ erg s}^{-1}$, is added to the disk bolometric luminosity, the total luminosity is roughly estimated as $2.4 \times 10^{40} \text{ erg s}^{-1}$ for $\alpha = 1$ (i.e., $i = 60^\circ$).

The observed X-ray luminosity requires a black hole mass of $> 150 M_\odot$ if the Eddington limit is satisfied. In contrast, the observed disk temperature of 1.45 keV is too high for the emission to be coming from a standard disk around such a massive black hole. In other words, the disk inner radius of 190 km is too small to be identified with the last stable orbit of a non-spinning black hole with $> 150 M_\odot$. If the obtained value of R_{in} were required to coincide with $6R_g$, then the Schwarzschild radius, $2R_g$, of this black hole would be only $\sim 64 \text{ km}$, which is equivalent to a black hole mass of $\sim 20 M_\odot$. Thus, the 2001 XMM-Newton observation of M81 X-9 clearly reproduces the “too high T_{in} ” problem described in § 1.

3.2. Analysis of the ASCA data in 1999

The flux and the MCD parameters obtained from the 2001 XMM-Newton data (§ 3.1) are very similar to those reported by La Parola et al. (2001), who analyzed the ASCA SIS data obtained on 1999 April 6 with the single power-law model and the single MCD model as introduced in § 3.1. In order to compare the ASCA and XMM-Newton spectra in a unified manner, we reanalyzed the same 0.5–10 keV ASCA SIS data with the same two-component model.

A right panel of figure 3 shows the ASCA SIS (SIS0 and SIS1) spectra with the best fit models. The results of this analysis are also shown in Table 1. The obtained best-fit parameters of the single power-law fit and the single MCD fit are consistent with those reported by La Parola et al. (2001). Although the single MCD model gave an acceptable fit with $\chi^2/(\text{d.o.f}) = 318/301$, addition of a power-law component improved the fit significantly in terms of an F -test, with $F(2, 301) = 20.8$ which corresponds to 99.99 %

significance. This two-component fit implies a 0.5–10 keV flux of $1.3 \times 10^{-11} \text{ erg s}^{-1} \text{ cm}^{-2}$ with the MCD component contributing $\sim 70\%$, and an unabsorbed 0.5–10 keV luminosity of $2.4 \times 10^{40} \text{ erg s}^{-1}$. The values of T_{in} and r_{in} have been estimated as $1.28_{-0.14}^{+0.12} \text{ keV}$ and $(220 \pm 50) \cdot \alpha \text{ km}$, respectively (Table 1). The spectral shape and the luminosity are thus almost the same, within errors, between the two observations with the different instruments.

3.3. Temperature profile of the optically thick disk

In addition to the “too high T_{in} ” problem, we encountered another problem in the spectral fit of M81 X-9. Although the two-component (MCD plus power-law) model apparently reproduces the spectra from the ASCA and the XMM-Newton observations, the power-law component exceeds the MCD component at energies below $\sim 1 \text{ keV}$, as shown in figure 3. Such a fit would be rather unphysical, since the power-law tail is generally considered as a consequence of inverse-Compton scattering of the MCD photons by high-energy electrons scattered around the accretion disk. Therefore, the hard-tail flux should not dominate that of the seed MCD, at least in the energy band below $2.8 kT_{\text{in}}$ which is the peak energy of a blackbody emission of temperature T_{in} . The apparent low-energy dominance of the power-law component suggests a subtle deviation of the accretion disk configuration from the standard one, in such a way that the softest end of the radially-integrated spectrum is more enhanced than the MCD model.

As described in §1, such a spectral change may arise if, e.g., the radiative efficiency of the inner disk region becomes reduced and the radial temperature gradient flattens; such effects can be quantified using the p -free disk model (Kubota & Makishima 2004). We hence fitted the MOS-1 and SIS data with the p -free disk model, and obtained the results presented in Table 1 and figure 3. In both the XMM-Newton and ASCA spectra, the p -free disk model is similarly, or even more, successful than the MCD+power-law fit. The values of p have been found as 0.60 ± 0.02 and $0.61_{-0.03}^{+0.04}$ with the *Newton* and ASCA data, respectively, in a very good mutual agreement. They are significantly smaller than the standard value of $p = 3/4$. The absorption column becomes somewhat higher than that implied by the single MCD fit. To reinforce the result, we simulated the spectrum by considering the possible systematic difference in the spectral index of $\Delta\Gamma \approx 0.1$ for the Newton off-axis sources (see figure 6 in Appendix). This difference was found to make the best fit value of p slightly smaller as $p = 0.58 \pm 0.02$, but it is within the statistic uncertainty.

Table 1. Spectral fitting parameters and derived quantities of M81 X-9.*.

Model	N_{H}^{\dagger}	Γ or p^{\ddagger}	T_{in} (keV)	r_{in} (km) §	M_{MCD} (M_{\odot}) §§	F_{X}^{\parallel}	$L_{\text{bol}}^{\#}$	$\chi^2/\text{d.o.f.}$
2001 April 22 (XMM-Newton)								
power-law	$2.88^{+0.11}_{-0.12}$	$1.96^{+0.03}_{-0.03}$				14.9		574.1/335
MCD	$0.75^{+0.08}_{-0.07}$		$1.35^{+0.02}_{-0.03}$	220 ± 4	30	13.0	21.0	427.4/335
MCD	$2.17^{+0.63}_{-0.42}$		$1.45^{+0.10}_{-0.14}$	160 ± 12	22	8.4	14.6	359.4/333
+power-law		$2.28^{+0.58}_{-0.35}$				5.1		
p -free disk	$1.70^{+0.19}_{-0.20}$	$0.60^{+0.02}_{-0.02}$	$1.72^{+0.11}_{-0.10}$	100 ± 20	—	13.5	$28.4^{\dagger\dagger}$	357.3/334
1999 April 06 (ASCA)								
power-law	$4.68^{+0.24}_{-0.23}$	$2.16^{+0.04}_{-0.04}$				13.9		453.3/301
MCD	$1.71^{+0.14}_{-0.14}$		$1.25^{+0.03}_{-0.03}$	260 ± 13	35	12.4	21.8	318.5/301
MCD	$3.18^{+2.76}_{-0.94}$		$1.28^{+0.12}_{-0.14}$	220 ± 50	29	8.5	16.1	297.8/299
+power-law		$2.35^{+1.95}_{-0.65}$				4.3		
p -free disk	$2.68^{+0.37}_{-0.38}$	$0.61^{+0.04}_{-0.03}$	$1.47^{+0.12}_{-0.10}$	140 ± 30	—	12.6	$28.3^{\dagger\dagger}$	298.3/300

* All quoted uncertainties are at the 90 % confidence limit.

\dagger Hydrogen column density for the photoelectric absorption, in units of 10^{21} cm^{-2} .

\ddagger The photon index for the power-law model, and the value of p for the p -free disk model.

\S An apparent innermost disk radius, assuming a distance of $D = 3.4 \text{ Mpc}$ and a disk inclination of $i = 60^\circ$.

$\S\S$ Black hole mass estimated by assuming that the true inner radius R_{in} coincides with $6R_{\text{g}}$.

Here the value of R_{in} is estimated by r_{in} with correction factors of $\xi = 0.41$ and $\kappa = 1.7$.

\parallel The absorption-uncorrected flux, in units of $10^{-12} \text{ erg s}^{-1} \text{ cm}^{-2}$.

$\#$ The bolometric luminosity, in units of $10^{39} \text{ erg s}^{-1}$.

$\dagger\dagger$ The 0.01-100 keV luminosity estimated from the best-fit model assuming isotropic emission.

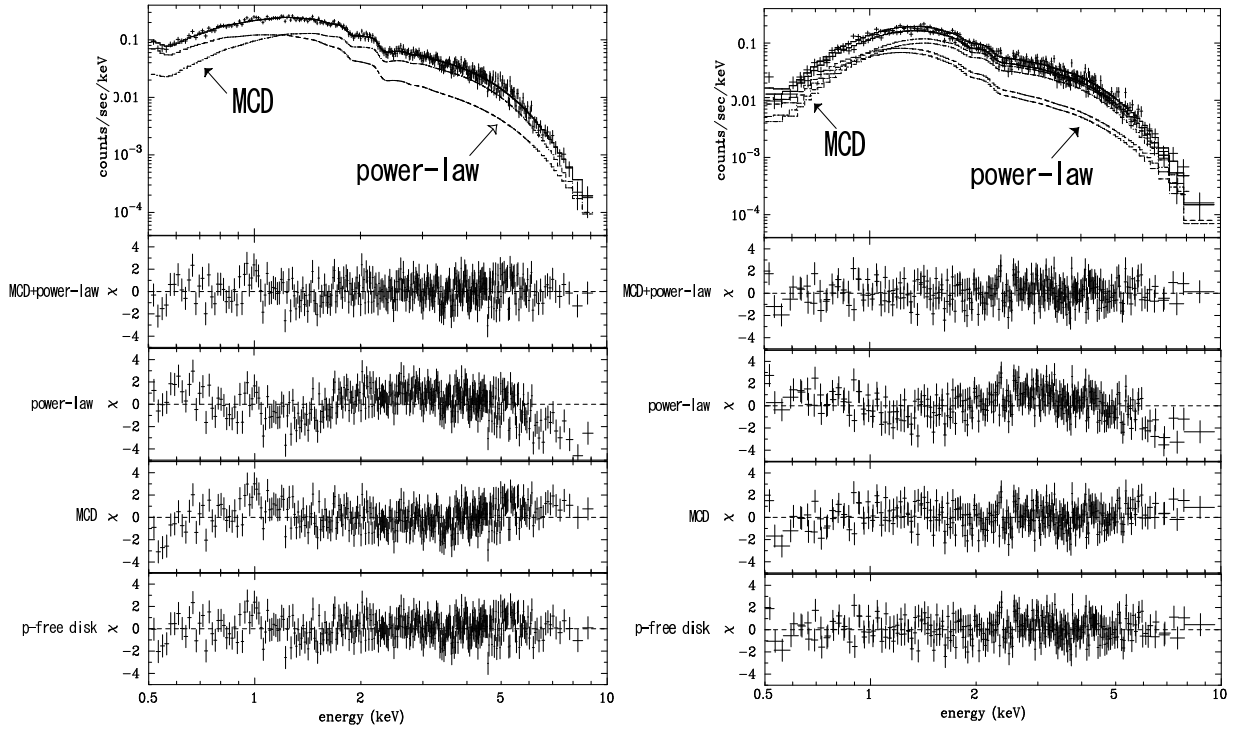


Fig. 3. The 0.5–10 keV spectra obtained with the XMM-Newton MOS-1 on 2001 April 22 (left), and with the ASCA SIS (SIS0 and SIS1) on 1999 April 6 (right). The best-fit MCD plus power-law models are superposed on the data. Bottom four panels show residuals between the data and the attempted models; from top to bottom, the MCD plus power-law, single power-law, single MCD, and the p -free disk models.

4. Discussion

Using the ASCA data acquired on 1999 April 6 and the XMM-Newton data on 2001 April 22, we studied the X-ray spectra of M81 X-9. On both occasions, the source exhibited typical disk dominated spectra, with very similar sets of spectral parameters including the bolometric luminosity of $\sim 2 \times 10^{40}$ erg s $^{-1}$. Combined with the power-law type spectra observed from this object at somewhat (a factor of ~ 2) lower luminosities (Ezoe, Iyomoto, Makishima 2001; Miller, Fabian, Miller 2004), our results reinforce the reports by La Parola et al. (2001) and Sugihō (2003) that M81 X-9 makes occasional transitions between the disk dominant and power-law dominant states.

In figure 4, we plot the present two measurements on the plane of L_{disk} vs. T_{in} after Makishima et al. (2000). For comparison, we also show results on several high- T_{in} ULXs, referring to Mizuno et al. (2001). Thus, the ULX data points, including those of M81 X-9, mostly fall on the apparent “super-Eddington” region, where L_{bol} significantly exceeds L_E which is calculated assuming standard accretion disks with $R_{\text{in}} = 6R_g$. This is just another representation of the “too high T_{in} ” problem. The figure also reveals the “variable r_{in} ” problem, because the ULX variations do not trace the dotted lines representing $L_{\text{bol}} \propto T_{\text{in}}^4$, but instead, behave approximately as $L_{\text{bol}} \propto T_{\text{in}}^2$ (or equivalently $r_{\text{in}} \propto T_{\text{in}}^{-1}$). Thus, we consider that M81 X-9 is subject to the same problems as described in § 1, although its variation is not very prominent on the diagram.

In order to solve these problems with the standard-disk interpretation of disk dominant spectra of luminous ULXs, we have adopted the slim-disk scenario as a working hypothesis, and analyzed the two data sets of M81 X-9 using the p -free disk model. As a result, the XMM-Newton and ASCA spectra have both been described by this model more successfully than by the traditional MCD model. Furthermore, the derived temperature profiles, $p = 0.60 \pm 0.02$ with XMM-Newton and $p = 0.61_{-0.03}^{+0.04}$ with ASCA, agree with each other, and are significantly smaller than the canonical value of $p = 3/4$ to be found with standard disks. In view of the theoretical prediction by Watarai et al. (2000) described in § 1, these results strongly suggest the presence of a slim disk in M81 X-9 on these occasions. In particular, the good agreement between the two different instruments significantly reduces the possibility that the deviation of p from $3/4$ is an instrumental artifact.

In figure 4, results on the Galactic BHB, XTE J1550 – 564, are also presented for comparison. At luminosities below $\sim 0.4L_E$, the data points of this BHB thus trace tightly a constant-mass (or $L_{\text{bol}} \propto T_{\text{in}}^4$) locus. At higher luminosities, however, the source starts deviating from this relation (Kubota & Makishima 2004), exhibiting the “variable r_{in} ” problem just like the ULXs. The same behavior has been observed from other BHBs as well, including 4U 1630 – 47 (Abe et al. 2005) and GRO J1655 – 40 (Kubota, Makishima, Ebisawa 2001). Kubota & Makishima (2004) named this characteristic

spectral state of BHBs *apparently standard regime*, because the spectra in this state resemble those from standard disks, except for significantly higher values of T_{in} . They showed that the RXTE spectra of XTE J1550 – 564 in this state can be described by the p -free model with $p < 0.75$.

Based on these considerations, we may presume that high- T_{in} ULXs and Galactic BHBs in the *apparently standard regime* have essentially the same spectral characteristics, which in turn are explained in terms of the formation of a slim disk; the only difference is that the ULXs are by an order of magnitude more luminous. Then, the first problem (too high T_{in}) can be solved at least qualitatively, because a slim disk appears significantly hotter than a standard disk. This interpretation also solves the second problem (variable r_{in}), because such a behavior is predicted by the slim disk theory (Watarai et al. 2000).

Then, how about the third problem, too high transition luminosity between the disk dominant and the power-law dominant states? Luminosity differences associated with ULX transitions (a factor of ~ 2 in the particular case of M81 X-9) are generally too small to identify the transitions with those between the low and high states of BHBs. In addition to the classical high-low transition, BHBs make transitions between the *standard regime* and the *apparently standard regime* at some critical luminosities, which are typically several tens of percents of L_E (Kubota et al. 2001; Kubota & Makishima 2004; Abe et al. 2005). Around this critical luminosity, yet another spectral state, called *very high* state (VHS; Miyamoto et al. 1991), sometimes appears. In this VHS, the spectrum becomes dominated by the power-law tail presumably due to Comptonization, even though the optically-thick disk emission underlies the spectrum Kubota et al. (2001; 2004). Kubota, Done, Makishima (2002) argued that the power-law dominant state of ULXs is analogous to the VHS of BHBs, rather than to their classical low state. This idea was also applied successfully to other power-law type ULXs (e.g., Stobbart et al. 2006). Then, the ULX transitions between the disk dominant and power-law (plus soft excess) type states can be regarded as analogous to the BHB transitions between the *apparently standard* state and the VHS. This solves the third problem, because the transition luminosity, $\sim 10^{40}$ erg s $^{-1}$, is now considered close to L_E , rather than to several percent of L_E .

Finally, let us touch on the black hole mass in M81 X-9. If the observed spectra are securely confirmed as emerging from the standard accretion disk, we can estimate the true inner radius, R_{in} , from the measured, r_{in} , through the corrections employed in §3.1. We can then identify R_{in} with the last stable orbit, to get an estimate on the black hole mass. However, now that the accretion disk in M81 X-9 has been confirmed to be significantly deviated from the standard disk, the correction from the apparent radius, r_{in} , to the true physical radius, R_{in} , would become highly model dependent. Even if we somehow derived R_{in} , we may not be justified in identifying it with $6R_g$ in an extreme slim disk condition. We thus do not attempt to

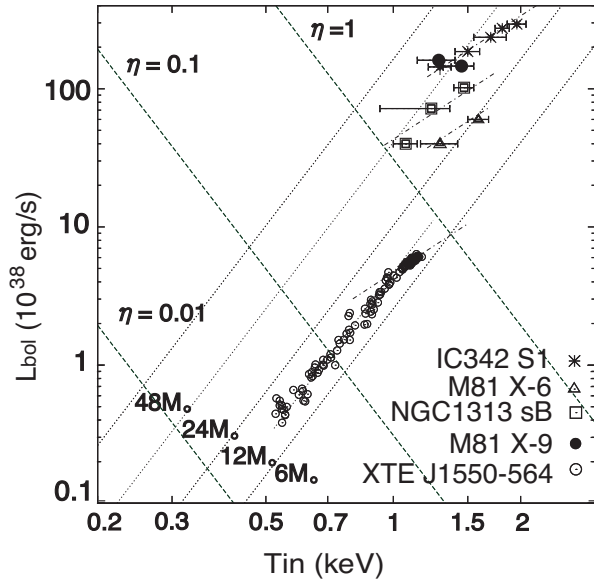


Fig. 4. The calculated L_{bol} plotted against T_{in} , both obtained from the MCD + power-law model. The dotted and dot-dashed lines represent the relations of $L_{\text{bol}} \propto T_{\text{in}}^4$ and $L_{\text{bol}} \propto T_{\text{in}}^2$, respectively. The dashed lines are the relation of $L_{\text{bol}} \propto T_{\text{in}}^{-4}$ (constant Eddington ratio $\eta \equiv L_{\text{bol}}/L_{\text{Edd}}$). All points of M81 X-9 refer to the present paper. Those of other ULXs, IC342 source 1, M81 X-6 and NGC 1313 Source B, are obtained with ASCA (Mizuno, Kubota, Makishima 2001; Makishima et al. 2000). The data of the Galactic BHB, XTE J1550 – 564, are obtained with *RXTE* (Kubota & Makishima 2004). The disk inclinations of the ULXs are assumed as 60° .

estimate the black hole mass based on the radius parameter obtained with the p -free fit.

Instead of using the radius parameter, a much safer argument on the black-hole mass can be made based on the luminosity. To keep the black hole mass to a normal stellar black hole of $\sim 10\text{--}20 M_\odot$, the observed luminosity is a factor 7–10 higher than its Eddington limit. Of course, such a highly super-Eddington luminosity could be possible from a theoretical viewpoint (e.g., Ohsuga et al. 2005). However, it would be more natural to consider that the object is radiating at close to its Eddington luminosity, considering that highly super-Eddington luminosities have not been observed from Galactic/Magellanic BHBs even if the disk deviate from the standard disk supposedly. In this case, the black hole mass is estimated as $\sim 100 M_\odot$. This exceeds a typical upper end of black hole mass which can reasonably form from models of single stellar collapse, and may suggest some kinds of merging (Ebisuzaki et al. 2001; Belczynski et al. 2004).

Acknowledgement

We are grateful to the XMM-Newton science operation center and the center for planning and information systems at ISAS/JAXA for making the data publicly available. We would like to thank Y. Maeda and K. Iwasawa

for their advices on analysis of off-axis sources. We also thank T. Tanaka and R. Miyawaki for helpful discussions. We are grateful to T. Mizuno for useful comments on this paper. A.K. is supported by a special postdoctoral researchers program in RIKEN. The present work is supported in part by Grant-in-Aid for Priority Research Areas, No.14079201 and No.1703011, from Ministry of Education, Culture, Sports, Science and Technology of Japan. It is also supported in part by the RIKEN’s budget on “Investigations of Spontaneously Evolving Systems”.

Appendix. The analysis of SNR G21.5-09

In order to examine the reliability of spectral and photometric results on highly off-axis XMM-Newton sources, we analyzed archival XMM-Newton data of the supernova remnant G21.5-09, acquired in off-axis and on-axis pointings. This source, one of Crab-like supernova remnants, has been observed many times with XMM-Newton for calibrating the mirror vignetting (Lumb et al. 2004). The observations were performed on 2000 April 7 for 17 ks, 2000 April 11 for 25 ks, and 2001 April 1 for 15 ks, with off-axis angle of $0'08$, $11'12$ and $13'02$, respectively. We analyzed these data sets in the same way as for M81 X-9. Figure 5 and Table 2 show the 1–10 keV spectra, and the parameters obtained from single power-law fits to them. Our results on the on-axis data are consistent with those reported by Warwick, Bernard, Bocchino (2001). As shown in Figure 6, the off-axis spectral parameters are consistent with the on-axis ones and the absorbed 1–10 keV flux is reproduced to within 10%.

Table 2. Spectral fitting parameters for G21.5-0.9 (1–10 keV).

offset	N_{H}^*	Γ^\dagger	F_{X}^\ddagger	$\chi^2/\text{d.o.f.}$
0'08	23.3 ± 0.6	1.86 ± 0.04	51.8	446.5/434
11'12	22.4 ± 0.6	1.82 ± 0.04	56.7	422.6/399
13'02	22.3 ± 1.0	$1.72^{+0.07}_{-0.06}$	55.5	298.8/323

* Hydrogen column density for the photoelectric absorption, in units of 10^{21} cm^{-2} .

† Photon Index Γ .

‡ The uncorrected absorption flux in the range of 1-10 keV, in units of $10^{-12} \text{ erg s}^{-1} \text{ cm}^{-2}$.

References

- Abe, Y., Fukuzawa, Y., Kubota, A., Kasama, D., & Makishima, K. 2005, PASJ, 57, 629
- Abramowicz, M. A., Czerny, B., Lasota, P., & Szuszkiewicz, E. 1988, ApJ, 332, 646
- Belczynski, K., Sadowski, A., Rasio, F. A., 2005, ApJ, 611, 1068
- Davis, S. W., Blaes, O. M., Hubeny, I., Turner, N. J. 2005, ApJ, 621, 372
- Ebisawa, K., Zycki, P., Kubota, A., Mizuno, T., Watarai, K. 2003, ApJ, 597, 780
- Ebisawa, K. et al. 1994, PASJ, 46, 375
- Ebisawa, K., Makino, F., Mitsuda, K., Belloni, T., Cowley, A. P., Schmidtke, P. C., & Treves, A. 1993 ApJ, 403, 684
- Ebisuzaki, T. et al. 2001, ApJ, 562, L19
- Ezoe, Y., Iyomoto, N., & Makishima, K. 2001, PASJ, 53, 69
- Georgiev, Ts. B., Bilkina, B. I., Tikhonov, N. A., & Karachentsev, I. 1991, A&AS, 89, 529
- Hirano, A., Kitamoto, S., Yamada, T., Mineshige, S., Fukue, J. 1995, ApJ, 446, 350
- Kubota, A., Done, C., & Makishima, K., 2002, MNRAS, 337, L11
- Kubota, A., Ebisawa, K., Makishima, K., & Nakazawa, K. 2005, ApJ, 631, 1062
- Kubota, A., & Makishima, K. 2004, ApJ, 601, 428
- Kubota, A., Makishima, K., & Ebisawa, K., 2001, ApJ, 560, 147
- Kubota, A., Tanaka, Y., Makishima, K., Ueda, Y., Dotani, T., Inoue, H., & Yamaoka, K. 1998 PASJ, 50, 667
- La Parola, V., Peres, G., Fabbiano, G., Kim, D. W., & Bocchino, F. 2001, ApJ, 556, 47
- Lumb, D. H., Finoguenov, A., Saxton, R., Aschenbach, B., Gondoin, P., Kirsch, M., & Stewart, I.M. 2004 [astro-ph/0403647]
- Makishima, K., Maejima, Y., Mitsuda, K., Bradt, H. V., Remillard, R.A., Tuohy, I.R., Hoshi, R., & Nakagawa, M. 1986, ApJ, 308, 635
- Makishima, K. et al., 2000, ApJ, 535, 632
- Miller, J.M., Fabian, A.C., & Miller, M.C. 2004, ApJ, 607, 931
- Mineshige, S., Hirano, A., Kitamoto, S., & Yamada, T. 1994, ApJ, 426, 308
- Mitsuda, K., et al. 1984, PASJ, 36, 741
- Miyamoto, S., Kimura, K., Kitamoto, S., Dotani, T., Ebisawa, K. 1991, ApJ, 383, 784
- Mizuno, T., Kubota, A., & Makishima, K. 2001, ApJ, 554, 1282
- Ohsuga, K., Mori, M., Nakamoto, T., & Mineshige, S. 2005, ApJ, 628, 368
- Okada, K., Dotani, T., Makishima, K., Mitsuda, K., & Mihara, T. 1998, PASJ, 50, 25
- Shakura, N.I., & Sunyaev, R.A. 1973, A&A, 24, 337
- Shimura, T., & Takahara, F., 1995, ApJ, 445, 780
- Stobbart, A.-M., Roberts, T. P., & Wilms, J. 2006, MNRAS, 368, 397
- Sugiho, M., 2003, Ph.D. thesis, The University of Tokyo
- Tanaka, Y., & Lewin, W. H. G. 1995, in X-ray Binaries, eds. W. H. G. Lewin, J. van Paradijs, and W. P. J. van den Heuvel (Cambridge University Press, Cambridge), p126
- Warwick, R.S., Bernard, J. P., & Bocchino, F., et al. 2001, A&A, 365, 248
- Watarai, K., Fukue, J., Takeuchi, M., & Mineshige, S. 2000, PASJ, 52, 133
- Watarai, K., Mizuno, T., Mineshige, S. 2001, ApJ, 549, 77

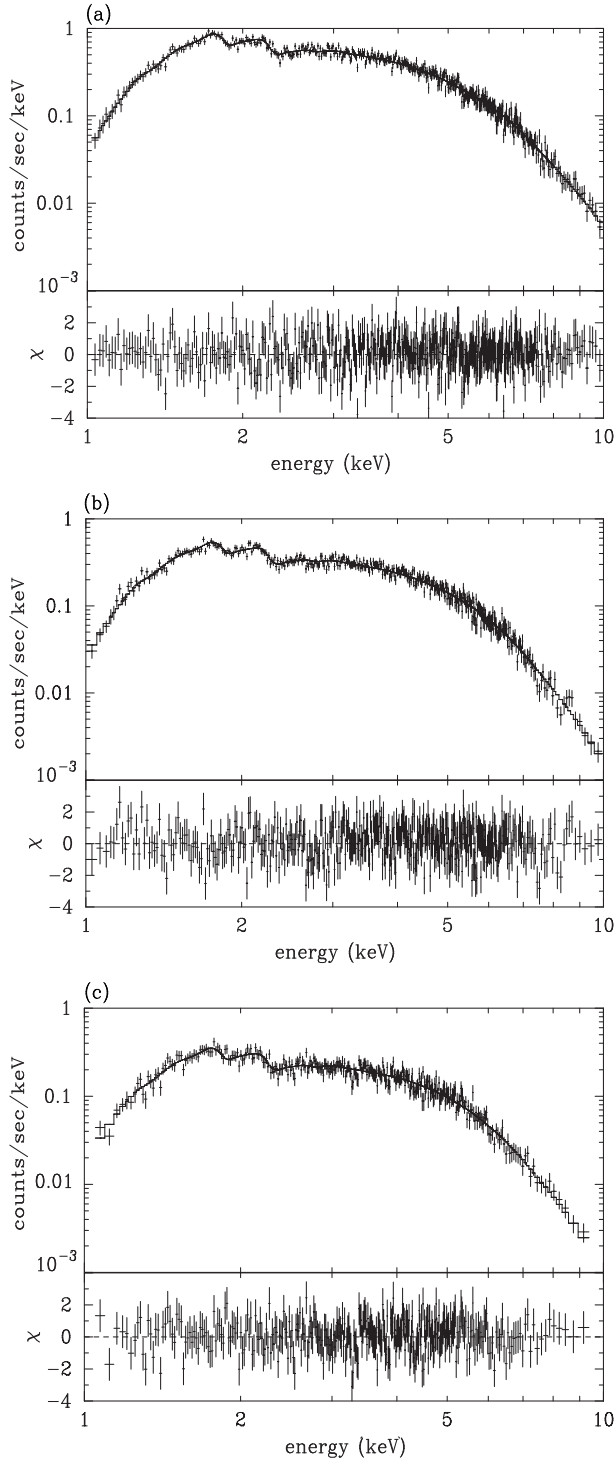


Fig. 5. MOS-1 spectra of G21.5–09 of acquired in; (a) an on-axis pointing, and off-axis pointings with offsets of (b) 11'.12 and (c) 13'.02. The best fit power-law model is superposed on the data.

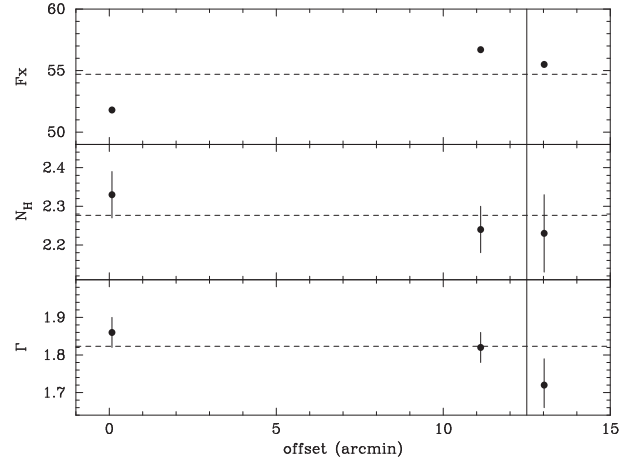


Fig. 6. The best-fit power-law model parameters of G21.5-09, plotted against the off-axis angle. From top to bottom, plotted are the 1–10 keV flux (in $10^{-11}\text{erg s}^{-1}\text{cm}^{-2}$), the hydrogen column density for the photoelectric absorption (in 10^{22}cm^{-2}), and the photon index. The line drawn at 12'.5 indicates the off-axis distance of M81 X-9 owing the 2001 April 22 observation.